

53-37
50431
125117

The Thermal Conductance of Solid-Lubricated Bearings at Cryogenic Temperatures in Vacuum

M. J. Anderson*

Abstract

The thermal conductance of Hertzian contacts is of great importance to cryogenic spacecraft mechanisms such as the Infra-Red Space Observatory (ISO) and the Far Infra-Red Space Telescope (FIRST). At cryogenic temperatures, cooling of mechanism shafts and associated components occurs via conduction through the bearings. When fluid lubricants are cooled below their pour points, they no longer lubricate effectively, and it is necessary to use low shear strength solid lubricants. Currently, only very limited low temperature data exists on the thermal conductance of Hertzian contacts in both unlubricated and lubricated conditions. This paper reports on measurements of thermal conductance made on stationary ball bearings under cryo-vacuum conditions. Quantitative data is provided to support the development of computer models predicting the thermal conductance of Hertzian contacts and solid lubricants at cryogenic temperatures.

Introduction

The thermal conductance of Hertzian contacts is important in cryogenic spacecraft applications. For example, cryogenically cooled mechanisms are integral components of the ISO and the FIRST. At cryogenic temperatures, the Hertzian contacts in ball bearings are often the only route by which heat can be extracted and thus enable the cooling of mechanism shafts and associated components to take place. Although extensive research has been carried out [1, 2] to measure the thermal conductances of metallic and non-metallic materials, often in loaded configurations, only very limited low temperature data exists on the thermal conductance of Hertzian contacts. In this work, the Hertzian contacts in a stationary ball bearing were investigated. Initially measurements were performed using an unlubricated bearing to confirm that the temperature dependence of the thermal conductance of Hertzian contacts was consistent with the bearing steel's thermal properties.

The unlubricated bearing measurements were followed by investigating the influence of solid lubricants on the thermal conductance of Hertzian contacts at room and at cryogenic temperatures. When fluid lubricants are cooled below their pour points, they no longer lubricate effectively and it is necessary to use low shear strength solid lubricants.

Research has shown that low shear strength solids are effective lubricants at both room and at cryogenic temperatures [4]. Two of the most widely used ball bearing solid lubricants, i.e. MoS₂ applied by RF magnetron sputtering, and lead applied by ion-plating, were studied. In addition to lubricant films, other coatings are frequently

* European Space Tribology Laboratory, AEA Technology, Warrington, Cheshire, UK

F7476346

applied, such as thin TiC coatings, which are used as adhesion barriers between contacting metallic surfaces.

This paper reports measurements of the radial thermal conductance made on ball bearings under cryo-vacuum conditions. Quantitative data is provided to support the development of computer models predicting the thermal conductance of Hertzian contacts, and solid lubricants, at cryogenic temperatures.

Basic Concept

A steady-state axial heat flow method was used to measure the radial thermal conductance across a bearing. Figure 1 illustrates the basic concept. Heat is supplied, at a constant rate, along a 304 stainless steel rod of uniform cross-section and known thermal conductivity and then across the test specimen to a heat sink. Temperature sensors enable measurements of the temperature gradients along the rod and across the test specimen to be made. Under steady-state conditions, the heat flow rate through the rod, known as the heat flux meter (HFM), equals that through the test specimen, provided there are no heat losses, e.g., by radiation. The mathematical expressions governing the heat flow rates through the HFM and test specimen, as functions of conductance and temperature gradient, can therefore be equated. The thermal conductance of the test specimen can then be determined by solving the resulting expression.

Under steady-state conditions, the heat flux (q_{HFM}) through the HFM is related to the conductivity (k) and dimensions of the HFM (cross-sectional area = A , and distance between temperature sensors = L) by the following expression:

$$q_{\text{HFM}} = (T_u - T_l) \cdot kA/L \quad (1)$$

T_u and T_l are as defined on Figure 2.

The heat flux through the bearing is determined by the bearing conductance (C) and is equal to that through the HFM. T_c and T_b denote the temperatures of the inner and outer raceways respectively. The outer raceway temperature is also equivalent to the nominal base temperature. The following expressions are obtained.

$$q_{\text{bearing}} = C \cdot (T_c - T_b) \quad (2)$$

Equating (1) and (2) gives

$$C = (T_u - T_l) / (T_c - T_b) \cdot kA/L \quad (3)$$

By measuring the temperature gradient across the bearing and at defined points on the HFM, the bearing conductance can be obtained using the above expression.

Experimental Details

Apparatus Design

Figure 2 is a schematic representation of the test bearing and HFM. The test specimen is a stationary angular-contact ball bearing. The outer raceway is attached to a copper support piece secured to the base. The base, in turn, is bolted to the 20 K cryopot of the ESTL vacuum Cryogenic Facility. The inner raceway is firmly fastened to the lower end of the HFM via an Oxygen Free High Conductivity (OFHC) Cu spacer which acts as a thermal short circuit. Such a precaution is essential to minimize temperature differences between the inner raceway and the bottom end of the HFM. A wire-wound resistive heater block is located within the upper portion of the HFM. Polyimide-insulated nichrome wire (resistivity = 34.4 Ohm/m) is used for the heater windings. The heater coil is located within the HFM so that heat radiated from the heater coil will be absorbed by the HFM, minimizing heat loss to the surrounding environment. Axial loading is accomplished by tensioning a steel wire running from the HFM to a spring system linked to a tension-load cell. The load cell enables the axial load to be measured and the springs give some degree of compliance to allow for the effects of thermal expansion and contraction. It is necessary to be able to alter the applied load so that the effect of load on bearing conductance can be quantified. In order to avoid the need for breaking the vacuum or warming the cryostat to room temperature, the load can be changed in-situ by rotating a manually operated linear motion drive connected to the upper end of the load cell.

Three locating balls, manufactured from PTFE, are situated between the heater block and the 20 K structure to prevent rotation of the HFM and contact assembly. The PTFE also thermally isolates the heater block from the cooling arm.

Silicon diode temperature sensors are located at each end of the HFM and on the bearing raceways as indicated on Figure 2. Three silicon diode temperature sensors are also spaced around the circumference of each raceway, and were defined as follows:

T_u	located on HFM and is the sensor closest to the heater coil
T_l	located on HFM and situated 3.0 cm from T_u .
T_{b1} to T_{b3}	attached on the outer raceway abutment faces of the bearing. These sensors also define the base temperature.
T_{c1} to T_{c3}	attached to the inner raceway abutment faces.

Radiative heat losses are minimized by insulating the surfaces of the HFM and by filling the space below the bearing with superinsulating material (aluminized mylar).

Test Bearings

The test bearings are specified as RA 8220 and were manufactured by RMB, Switzerland. The bearing details are shown in Table 1.

Table 1 Bearing Details

Raceway Material	440C stainless steel
Ball Material	440C stainless steel
Outer Raceway Diameter	22.0 mm
Bore	8.0 mm
Width	7.0 mm
Ball Diameter	3.969 mm
Ball Complement	7
Conformity	1.14
Contact Angle	15 degrees

Table 2 summarizes the coating processes applied to the rolling elements and defines the cage materials.

Table 2 Details of Bearing Coatings and Lubrication

Bearing ID	Ball Coating	Raceway Coating	Cage Material
Unlubricated	None	None	303 stainless steel ¹
Lead	None	Ion-plated lead	Lead/bronze
MoS ₂	MoS ₂	MoS ₂	RT/duroid 5813 ²
TiC Balls	CVD TiC	None	303 stainless steel ¹

¹ Cage unlubricated.

² RT/duroid 5813 is an MoS₂/PTFE/glass fiber composite manufactured by the Rogers Corporation, USA

The lead film was deposited, at ESTL, by lead-ion plating and the MoS₂ films were deposited by RF magnetron sputtering, also at ESTL. Estimations of film thickness were made using an X-ray fluorescence technique and the typical MoS₂ film thickness on the bearing inner raceway was 0.8±0.2 microns and 0.20±0.03 microns on the balls. For the lead films, a typical thickness was 0.7±0.1 microns on the inner raceway.

The TiC coating (thickness = 3 microns, according to CSEM literature) was applied to the balls by CSEM, Switzerland, by their proprietary chemical vapor deposition technique.

The following Table summarizes the load and contact stress conditions under which the bearings were tested.

Table 3 Load and Contact Stress Conditions

Load (N)	Mean Hertzian Contact Stress	
	(Inner Raceway, MPa)	(Outer Raceway, MPa)
0	0	0
10	614	491
20	769	615
40	962	769
60	1094	875
80	1198	958

Additionally, it should be noted that the bearings were not run-in prior to testing.

Experimental Errors

Experimental errors arise from the errors in the measurements of thermal gradients across the bearing and along the HFM. Experimental errors are governed by the accuracy of the temperature sensors (± 0.5 K at room temperature and ± 0.2 K at 20K). Further errors result from heat loss and in the dimensions of the HFM. A summary of experimental errors is now presented.

Room Temp: HFM calibration errors are of the order of $\pm 25\%$, and the dimensional tolerances give the error in $L = \pm 2\%$, and the error in $A = \pm 1\%$.

At 48 mW heater power, typical temperature differentials across the bearing were 2 to 4K. As the sensors are only accurate to ± 0.5 K, experimental errors on temperature measurements are, respectively, $\pm 50\%$ and $\pm 25\%$. Combining this error with HFM calibration and dimensional errors gives a maximum experimental error of approximately $\pm 80\%$.

Increasing the heater power to 180 mW resulted in larger temperature gradients, and hence the measured temperature difference errors were reduced by a factor of 4 to 5, i.e., errors are of the order of $\pm 10\%$. The resulting experimental errors, including HFM calibration and dimensional errors, were of the order of $\pm 40\%$ to $\pm 50\%$.

Cryogenic Temperatures: The improved sensitivities of the temperature sensors, at cryogenic temperatures, resulted in HFM calibration errors of $\pm 10\%$. Combining these with the dimensional errors and the measured temperature gradients give typical experimental errors of less than $\pm 30\%$. At 20 K baseplate temperatures, maximum errors can be as great as $\pm 70\%$ if the temperature differentials are less than 1 K.

Results

HFM Calibration

The HFM was manufactured from 304 stainless steel and it was calibrated by applying a known quantity of power to the HFM heater, and measuring the temperature gradient along the HFM. Equation (1) was used to obtain the thermal conductivity, k , of the HFM material. Figure 3 shows the temperature dependence of the HFM material's

thermal conductivity. The conductivity varied non-linearly, from 6 W/m/K at 35 K, to 22 W/m/K at room temperature. The values plotted on this graph were used for the subsequent calculations of the bearing thermal conductance at a given temperature.

Results

The graphs of thermal conductance, at cryogenic temperatures, show data for baseplate temperatures of, nominally, 20 K and 50 K. At each baseplate temperature, two levels of power (48 mW, denoted by (1) in Tables 4 to 7, and 180 mW, denoted by (2)) were applied to the HFM heater, which varied the thermal gradients along the HFM and across the bearing. This resulted in two different values of the mean bearing temperature for a given baseplate temperature. The mean bearing temperatures are given in Tables 4 to 7. For cryogenic temperatures, the first two columns relate to a baseplate temperature of 20 K, and the following two columns to a baseplate temperature of 50 K.

The thermal conductance results, for zero applied axial load and for an 80 N axial load, are summarized in the Tables 4 to 7. The Tables summarize data from tests conducted at 293 K and at cryogenic temperatures.

Table 4 Thermal Conductance ($\times 10^{-3}$ W/K) of an Unlubricated Brg

Load (N)	Temp (K)	Cryogenic Temp (K)				Room Temp (293 K)	
		25	45	55	65	(1)	(2)
0		0.19	0.21	0.88	0.65	5.88	4.11
80		2.00	5.28	5.64	6.42	31.5	23.2

Table 5 Thermal Conductance ($\times 10^{-3}$ W/K) of a Lead lubricated Brg

Load (N)	Temp (K)	Cryogenic Temp (K)				Room Temp (293 K)	
		27	40	46	57	(1)	(2)
0		1.41	-	1.44	3.77	-	12.1
80		3.27	4.32	6.42	8.43	35.1	29.4

Table 6 Thermal Conductance ($\times 10^{-3}$ W/K) of an MoS₂ lubricated Brg

Load (N)	Temp (K)	Cryogenic Temp (K)				Room Temp (293 K)	
		35	50	55	65	(1)	(2)
0		0.35	0.59	1.41	1.18	4.38	6.47
80		1.92	5.02	3.76	-	18.1	18.1

Table 7 Thermal Conductance ($\times 10^{-3}$ W/K) of a Brg fitted with TiC-coated Balls

Load (N)	Temp (K)	Cryogenic Temp (K)				Room Temp (293 K)	
		35	52	65	75	(1)	(2)
0		0.87	1.76	1.25	2.5	10.9	-
80		4.65	6.40	7.51	7.51	13.9	24.5

Examination of the data showed that, at room temperature, the thermal conductance of the unlubricated bearing was 0.03 W/K at an 80 N axial load. A decrease of approximately an order of magnitude was measured over the temperature range from room temperature to 20 K (baseplate temperature) and the 50 K results were intermediate. At all test temperatures, the effect of the lead film was to increase the thermal conductance of a bearing by up to 30%. An MoS₂ film caused the thermal conductance to be up to 20% less than that for an unlubricated bearing. The thermal conductance of the bearing fitted with TiC-coated balls was comparable, at room and at cryogenic temperatures, with the thermal conductance of the unlubricated bearing containing steel balls.

The bearing thermal conductance varied non-linearly with applied axial load. A typical example of Thermal Conductance vs Axial Load is shown in Figure 4. Note that the thermal conductance was not zero when no axial load is applied.

Discussion

General Comments

The bearing conductance at zero applied axial load is not zero as heat transfer occurs across the bearing by radiation at room temperature and, at room and cryogenic temperatures, via the thermal path presented by ball raceway contacts due to the finite cage weight.

The thermal conductances for the bearings have been plotted against the Hertzian contact area per ball at the ball/inner raceway (Figures 5 to 9). Figure 5 shows the room temperature data for all bearing/coating combinations tested. In the graphs, at cryogenic temperatures, a correction has been made for the change in Young's Modulus (assumed to increase by 10%[2]). In general, Figures 6 to 9 are linear within experimental error, thus indicating that the thermal conductance of a solid lubricated or unlubricated bearing is proportional to the Hertzian contact area, and hence proportional to load^{2/3}.

Some anomalous points were found, in which the measured conductance values deviated from the best fit line through the points, and the values are also outside the experimental errors predicted. This additional error is consistent with errors arising from ball load distribution. Assuming 6 balls were loaded, the error is of the order of between 10% and 20%, as corresponding reductions, in the Hertzian contact areas, also occur at the outer raceway contacts.

Unlubricated Bearing

At cryogenic temperatures, the bearing thermal conductance is less than it is at ambient temperatures as a consequence of the reduced thermal conductivity of the bearing steel, as discussed in References 1 and 2. A similar decrease was obtained in the material used to fabricate the HFM.

Lead Lubricated Bearing

The thermal conductance for the lead-lubricated bearing exceeds that of the unlubricated bearing. In the unlubricated bearing, conduction takes place only through the asperities of the Hertzian contacts at the ball/race interfaces. In the lead-lubricated bearing, thermal conduction can now occur via the Hertzian contact and through any additional thermal paths created by the contact asperity gap-filling properties of the lead film.

MoS₂-Lubricated Bearing

Typically, non-metallic materials exhibit relatively low thermal conductivities in comparison with metals [2]. A thin film of MoS₂ applied between contacting asperities would therefore act as an insulating layer and reduce the thermal conductance of the bearing. The results, at ambient and at cryogenic temperatures, confirm that the thermal conductance of an MoS₂-lubricated bearing is less than that of an unlubricated bearing.

Unlubricated Bearing Fitted with TiC-Coated Balls

The thermal conductance results obtained at cryogenic temperatures for the bearing fitted with TiC-coated balls are comparable to the corresponding data obtained for the unlubricated bearing. Such a result is expected, as the thermal conductivity of TiC is similar to that of steel [5].

Effect of Bearing Rotation

Although the experimental technique described in this report focuses on a stationary bearing, the results can be applied to slowly rotating bearings. It was shown theoretically by Holm [3], and also experimentally by Stevens and Todd [6] that the heat flow path is essentially unchanged between a stationary and a slow moving contact. In a stationary bearing, the heat flow path is dependent on the geometries of the Hertzian contacts. The regions of the bearing raceways between contacts only play a minor role in the heat flow process. As a bearing rotates, the heat flow path will be altered by thermal dissipation in the inter-contact regions. At slow speeds the change is not significant, but at higher speeds, the heat generated at a contact will not have dissipated before the arrival of the next contact. The heat flow characteristics will therefore change and alter the thermal conductance of the bearing. Stevens and Todd found that the heat flow characteristics, and thus the thermal conductance, of their test bearings remained unchanged below rotation rates of 100 rpm. The time taken for heat to dissipate is dependent on the rotation rate, the specific heat capacity and inversely proportional to the thermal conductivity (Reference 7 contains details of the calculation). As temperature is decreased from room temperature to 20 K, the heat capacity of steels decreases by at least an order of magnitude more than the thermal conductivity. Heat can therefore be expected to dissipate more rapidly with

decreasing temperature. The thermal conductance measurements carried out on stationary bearings are thus representative of slowly rotating bearings.

Extrapolation of Thermal Conductance Data

Changes in thermal conductance, due to applying solid lubricants, are of the order of $\pm 20\%$. In applications requiring the thermal conductance of a bearing to be maximized, then lead lubrication provides an improvement over MoS_2 lubrication. Fitting with TiC balls and applying an MoS_2 coating to the bearing is unlikely to reduce the thermal conductance to a limit which is far below that of MoS_2 lubrication alone. It must be noted, however, that in any application, the benefits gained by any particular method of solid lubrication to the thermal conductance must be considered along with the torque and duty requirements of the bearings.

Figure 10 can be used to predict the thermal conductance for a given coating/temperature combination. Extrapolation of the results to bearings of differing dimensions must be performed with caution, although any deduced data may be sufficient for a first approximation.

Conclusions

The measured changes in the thermal conductances of Hertzian contacts in ball bearings, as a function of temperature, is primarily related to the changes in bulk material properties. The influence of lubricant and TiC coatings is a secondary effect.

Ion-plated lead, applied to the raceways of a 440C bearing, increased the thermal conductance by 20%, at room temperature and 20 K. The increase was attributed to the gap-filling properties and the relatively high thermal conductivity of the lead film.

Sputtered MoS_2 films, applied to the balls and raceways, reduced the thermal conductance of the bearing by up to 35%, and was due to the MoS_2 film acting as an insulating layer.

TiC coatings, on the balls, did not change the bearing thermal conductance as the thermal conductivity of TiC is similar to that of steel.

The thermal conductance, in all test cases, increased non-linearly with applied axial load, and was found to be directly proportional to the Hertzian contact area.

The finite thermal conductance values, measured at zero applied axial load, were due to the thermal path through the ball/raceway contacts under the weight of the cage and, at room temperature, radiative heat transfer.

References

1. Gould, S. G. "The Thermal Conductance of Solids and Pressed Contacts at Very Low Temperatures." ESTL/TR/80, 1988.
2. Reed, P. R. and A. F. Clark. Materials at Low Temperatures, American Society for Metals, 1983.
3. Stevens, K. T. and M. J. Todd. "Thermal Conductance Across Ball Bearings In Vacuum," ESA Tribology/1, 1979.
4. Gould, S. G. and E. W. Roberts. "The In-Vacuo Torque Performance of Dry-Lubricated Bearings at Cryogenic Temperatures," 23rd Aerospace Mechanisms Symposium, May 1989.
5. Kaye, G. W. C. and T. H. Laby. Tables of Physical and Chemical Constants, Longman, 1973.
6. Holm, R. Electrical Contacts. Springer Verlag, 4th Edition, 1967.
7. Rowntree, R. A. "Metallurgical Phase Transitions in the Rubbing of Steels," PhD Thesis, University of Leicester, UK, 1982

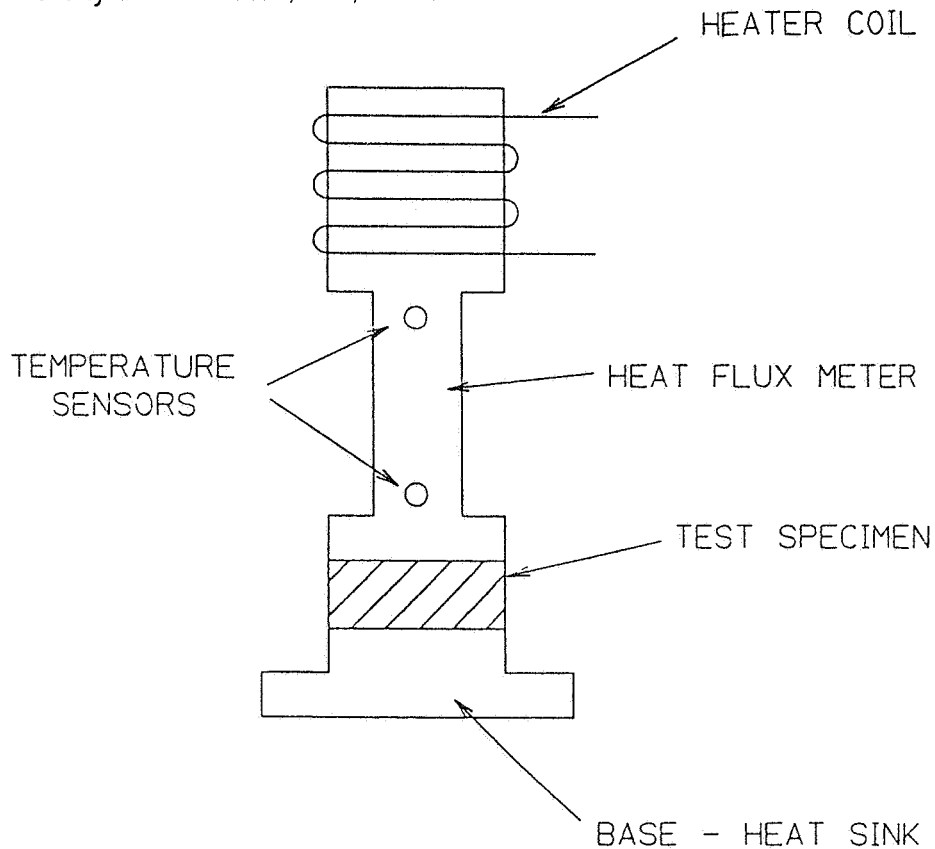


Figure 1 DESIGN CONCEPT

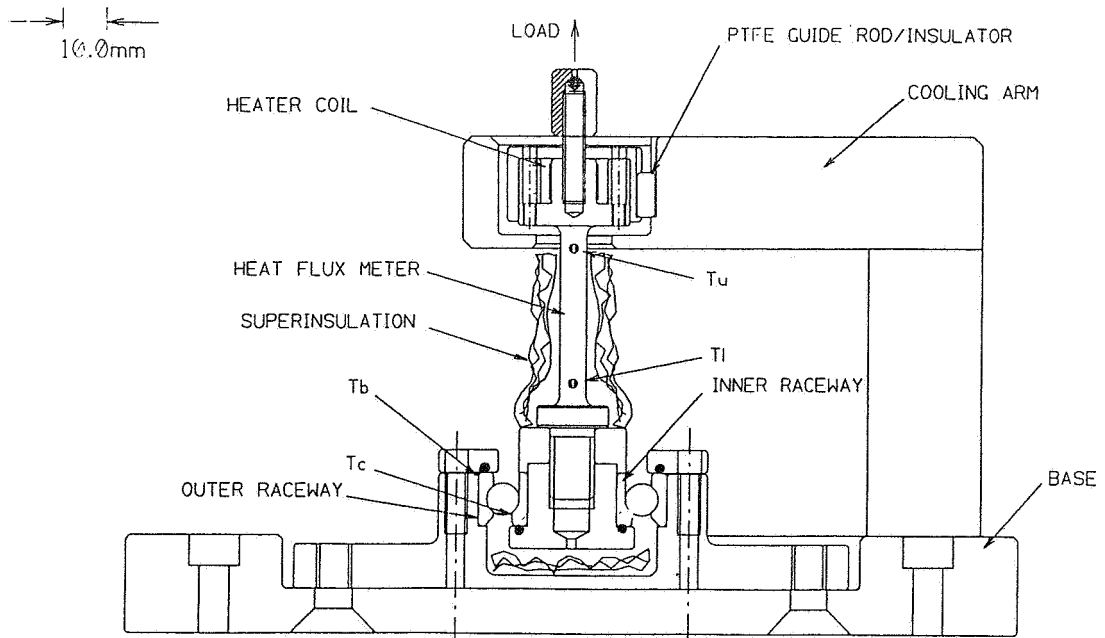
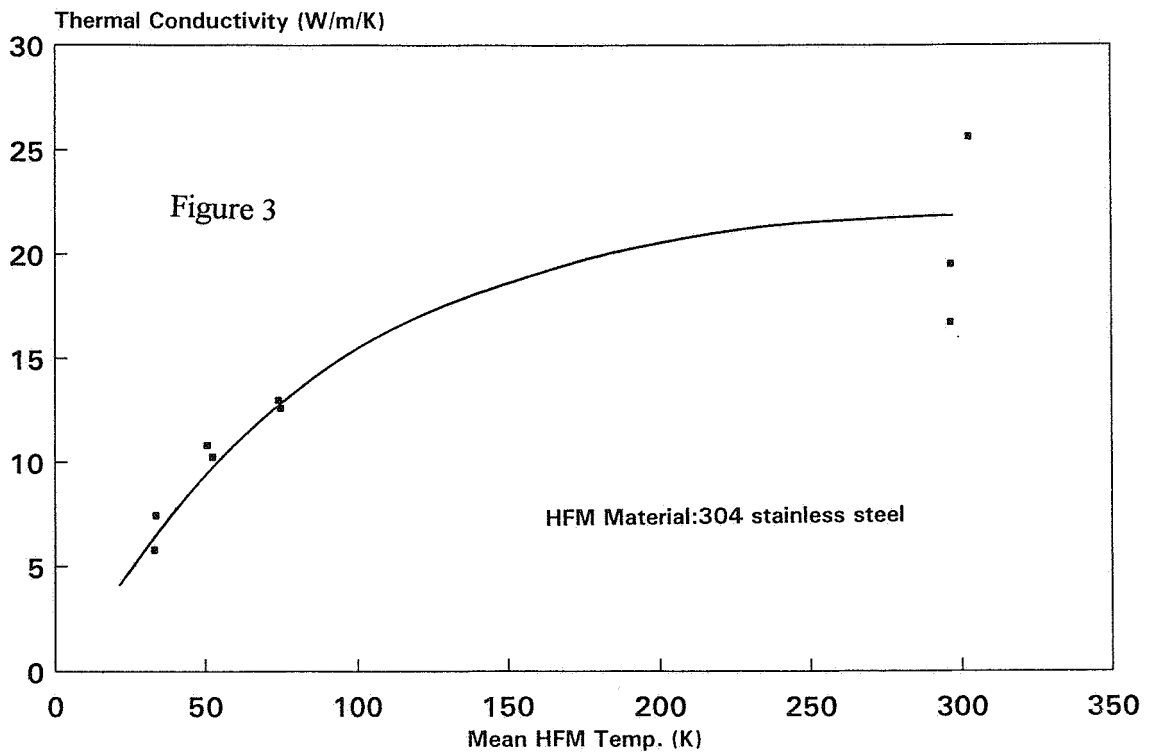


Figure 2 CRYO-THERMAL CONDUCTANCE RIG
ED 20 BEARING TEST SET UP

CRYOGENIC THERMAL CONDUCTANCE EXPT. Thermal Conductivity of HFM vs Temp.



CRYOGENIC THERMAL CONDUCTANCE EXPT.
Thermal Conductance vs Axial Load
ED8 Bearing (440C), Cryogenic Temp.

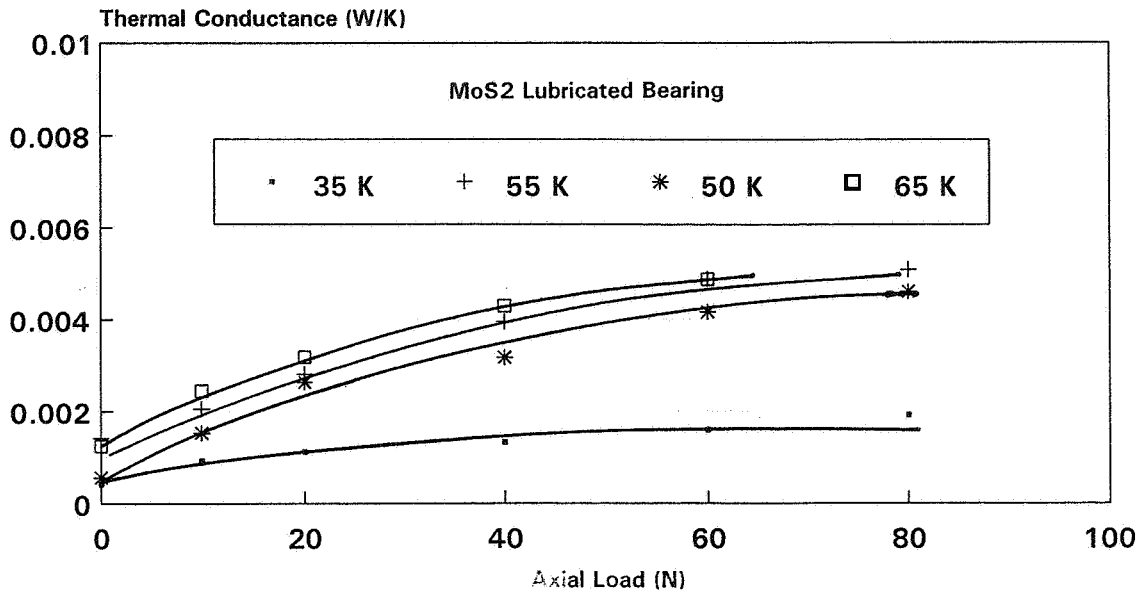


Figure 4

CRYOGENIC THERMAL CONDUCTANCE EXPT.
Thermal Conductance vs Contact Area
ED8 Bearing (440C), room temp.

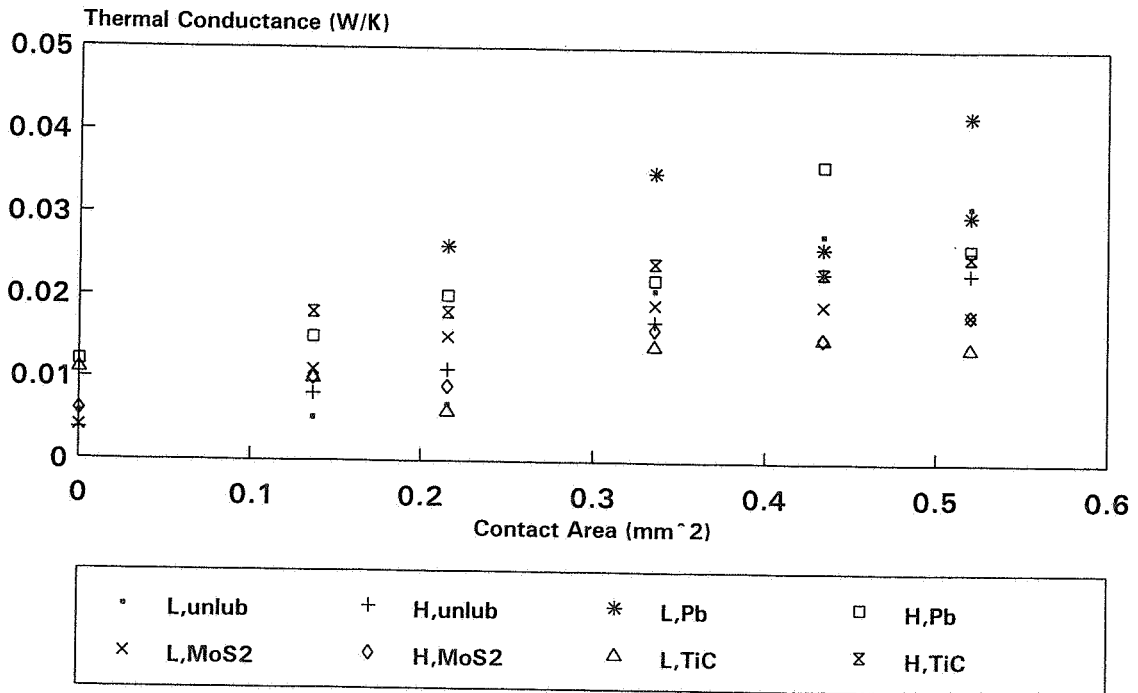


Figure 5

CRYOGENIC THERMAL CONDUCTANCE EXPT.
Thermal Conductance vs Contact Area
ED8 Bearing (440C), cryogenic temp.

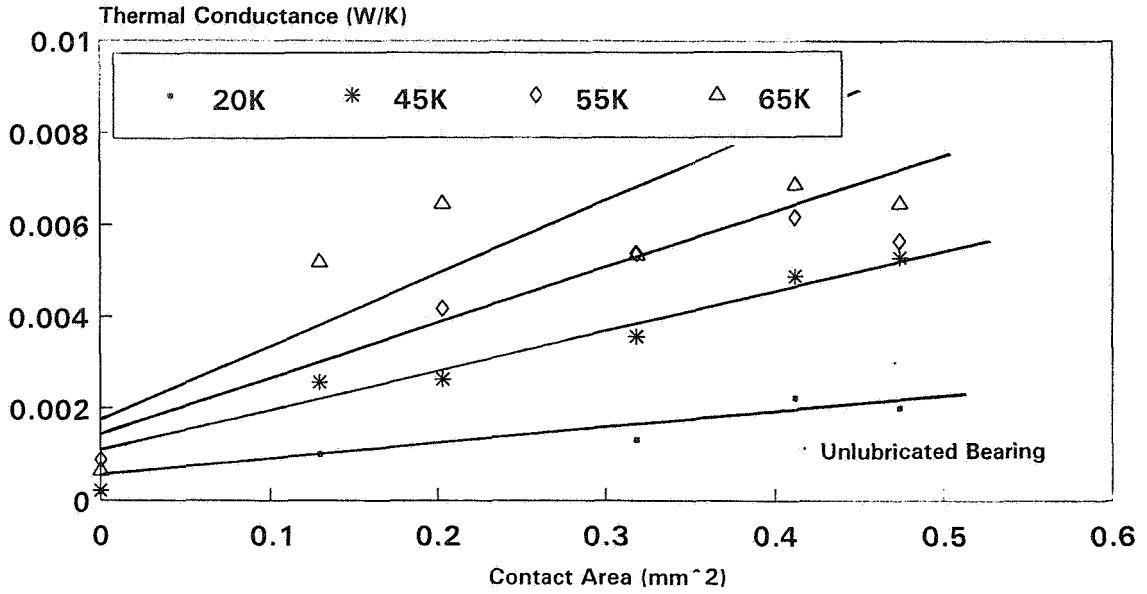


Figure 6

CRYOGENIC THERMAL CONDUCTANCE EXPT.
Thermal Conductance vs Contact Area
ED8 Bearing (440C), cryogenic temp.

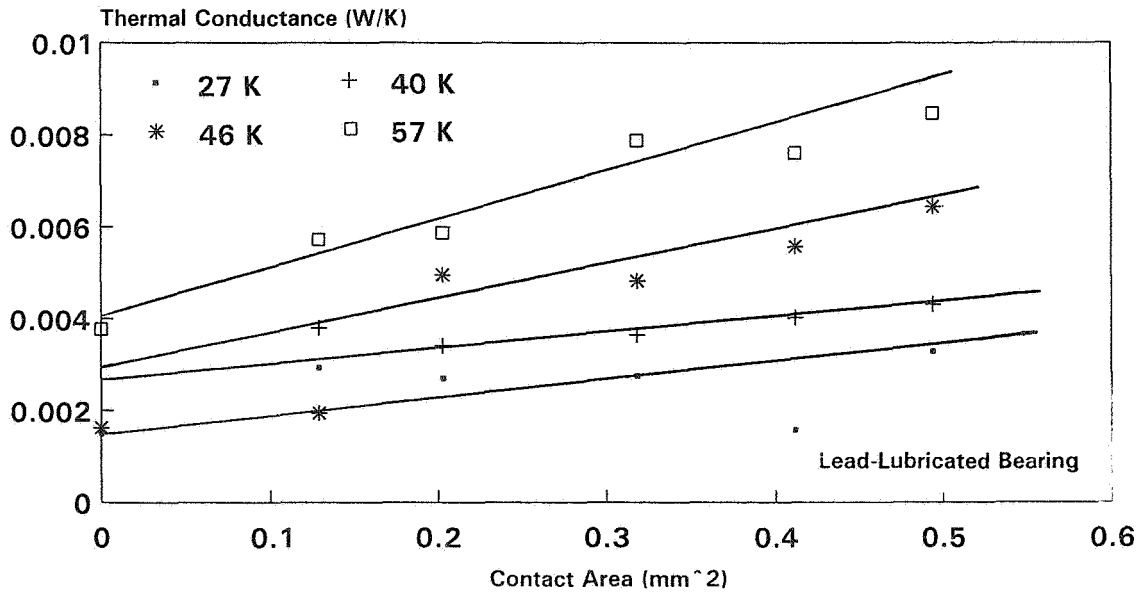


Figure 7

CRYOGENIC THERMAL CONDUCTANCE EXPT.
Thermal Conductance vs Contact Area
ED8 Bearing (440C), cryogenic temp.

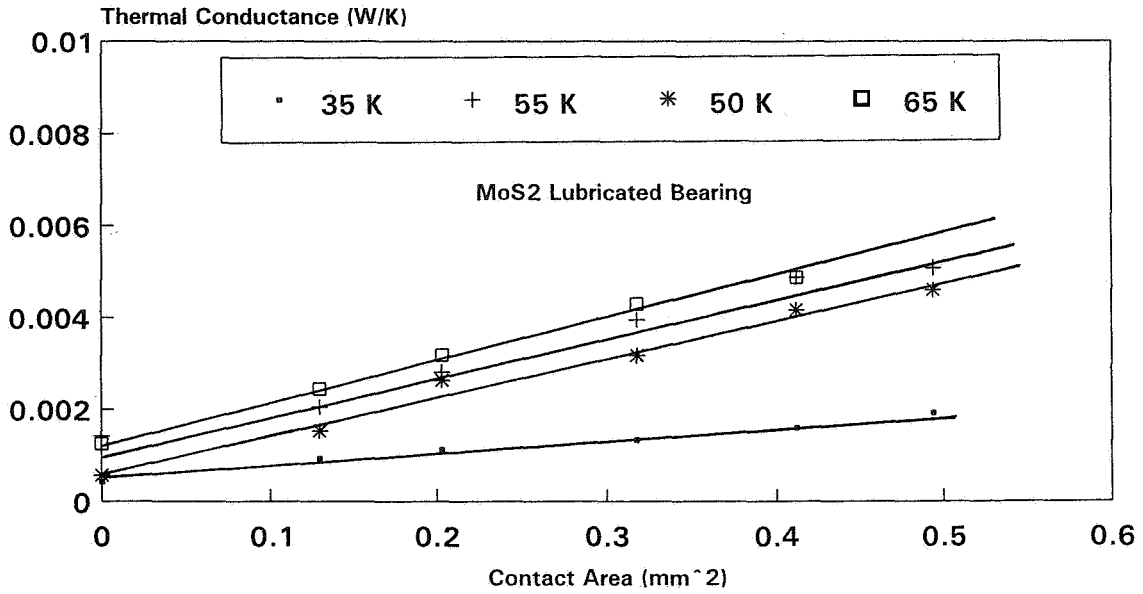


Figure 8

CRYOGENIC THERMAL CONDUCTANCE EXPT.
Thermal Conductance vs Contact Area
ED8 Bearing (440C), cryogenic temp.

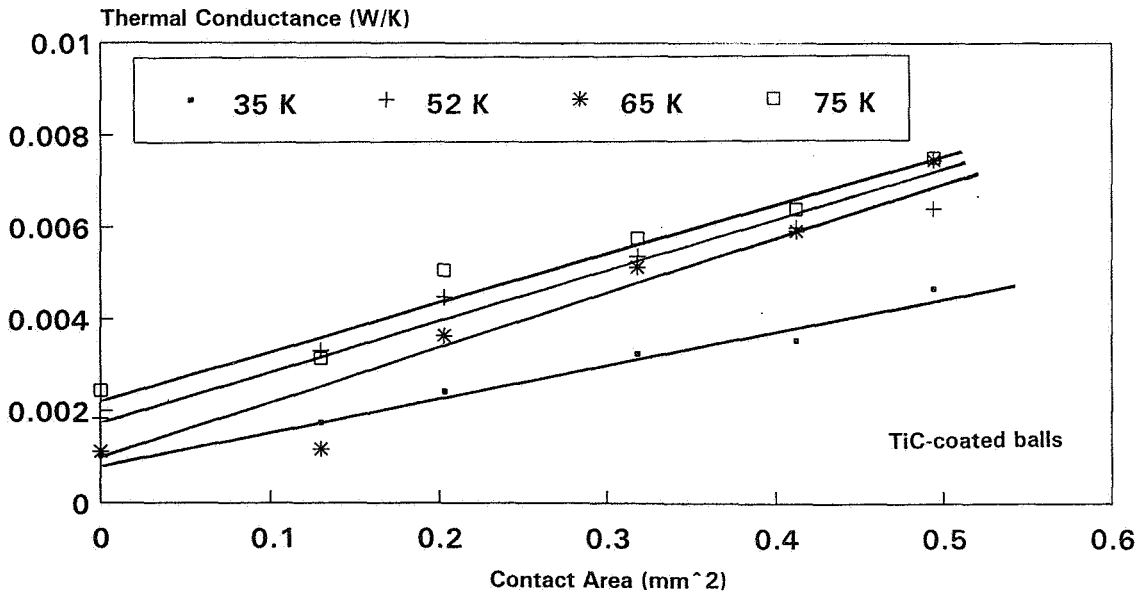


Figure 9

BEARING THERMAL CONDUCTANCE AS FUNCTION OF TEMPERATURE (IN VACUO)

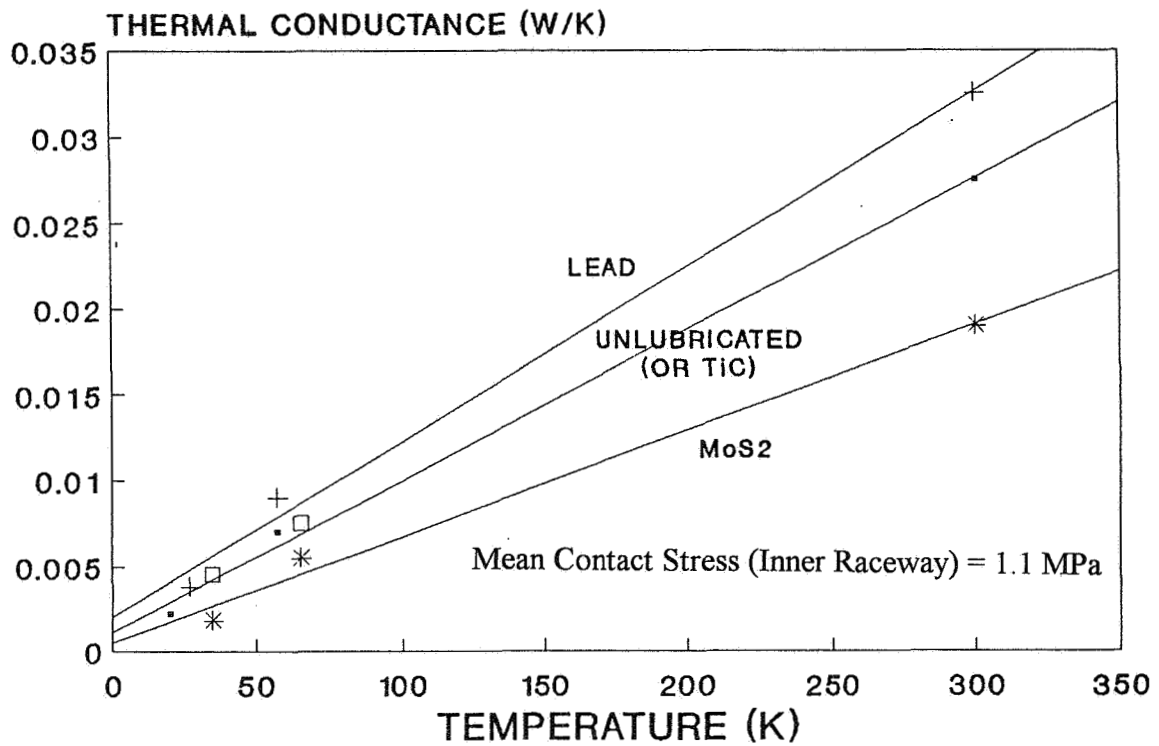


Figure 10